32, 2443-2445.
(34) Walker, J. A.; La Mar, G. N. *Ann. N.Y. Acad. Sci.* **1973**, *206*, 328-348.
(35) Falk, J. E. "Porphyrins and Metalloporphyrins"; Elsevier: Amsterdam, 1964; p 179.
(36) Collman, J. P.; Reed, C. A. *J. Am. Chem. Soc.* **1973**, *95*, 2048-2049.
(37) Epstein, L. M.; Straub, D. K.; Maricondi, C. *Inorg. Chem.* **1967**, *6*, 1720-1724.
(38) Evans, D. F. *J. Chem. Soc.* **1959**, 2003-2005.

Electron Exchange Kinetics of $[Fe_4S_4(SR)_4]^{2-}/[Fe_4S_4(SR)_4]^{3-}$ and $[Fe_4Se_4(SR)_4]^{2-}/[Fe_4Se_4(SR)_4]^{3-}$ Systems. Estimates of the Intrinsic Self-Exchange Rate Constant of 4-Fe Sites in Oxidized and Reduced Ferredoxins

John G. Reynolds, Catherine L. Coyle,[1] and R. H. Holm*

Contribution from the Department of Chemistry, Stanford University, Stanford, California 94305. *Received November 8, 1979*

Abstract: The electron self-exchange kinetics for the systems $[Fe_4S_4(SR)_4]^{2-,3-}$ (R = CH_2Ph, p-C_6H_4Me) and $[Fe_4Se_4(S$-p-$C_6H_4Me)_4]^{2-,3-}$ have been determined by general line shape analysis of exchange-broadened ^1H NMR spectra in acetonitrile solution. Reactions are second order, first order each in oxidized and reduced clusters, and at 300-304 K rate constants fall in the interval 10^6-10^7 M^{-1} s^{-1}, placing them among the faster inorganic self-exchange systems. For the $[Fe_4S_4(S$-p-$C_6H_4Me)_4]^{2-,3-}$ electron exchange $k_{301K}(obsd) = 2.8 \times 10^{-6}$ M^{-1} s^{-1} with activation parameters $\Delta H^{\ddagger} = 3.6$ kcal/mol and $\Delta S^{\ddagger} = -17$ eu. The structural reorganization energy of Fe_4S_4 cores upon passing from a compressed tetragonal to an elongated tetragonal geometry via a proposed T_d transition state in an outer-sphere process is estimated to be $\Delta G^{\ddagger}_{reorg} \sim 1.4$ kcal/mol. The rate constants are the best current estimates of the intrinsic values for the $[Fe_4S_4(S$-$Cys)_4]$ redox sites of ferredoxins in the couple Fd_{ox}/Fd_{red}, for which $[Fe_4S_4(SR)_4]^{2-}$ and $[Fe_4S_4(SR)_4]^{3-}$ serve as synthetic analogues of the sites of oxidized and reduced proteins, respectively. The "slow" electron self-exchange rates on the NMR time scale between oxidized and reduced forms of proteins containing one 4-Fe site can now be primarily attributed to kinetically retarding steric influences of protein structure rather than intrinsically slow reactions of the sites themselves.

Introduction

The principal physiological functions of that class of iron-sulfur proteins known as ferredoxins (Fd) is electron transfer, wherein these proteins serve as components of electron-transport chains coupled to a wide variety of "ferredoxin-dependent" oxidoreductases.[2] In this function many ferredoxins appear to operate through the Fd_{ox}/Fd_{red} couple

$$[Fe_4S_4(S\text{-}Cys)_4]^{2-}\ (Fd_{ox}) + e^- \rightleftharpoons [Fe_4S_4(S\text{-}Cys)_4]^{3-}\ (Fd_{red}) \quad (1)$$

in the case of proteins containing 4-Fe sites. Required information for an ultimately satisfactory interpretation of the functional operation of ferredoxins is accurate values of potentials and electron exchange rates and identification of those factors, intrinsic and extrinsic to the redox site, which significantly influence these quantities. One set of such factors which is expected to affect both equilibrium and kinetic aspects of protein behavior are the structures of the oxidized and reduced forms. Although the structures of *Peptococcus aerogenes* Fd_{ox}[3] and the reduced "high-potential" protein from *Chromatium*[3bc] (HP_{red}), which contain isoelectronic 4-Fe sites, are rather well defined from protein crystallography, no structure of a Fd_{red} protein is available. Further, no electron-exchange rates for Fd_{ox}/Fd_{red} are available other than certain estimated values (vide infra). Our approach to elucidation of the operation of Fd 4-Fe redox sites utilizes well-characterized synthetic analogues of these sites.[4,5]

Extensive physicochemical investigations of the oxidized cubane-type clusters $[Fe_4S_4(SR)_4]^{2-}$ [4-10] and their one-electron reduction products, $[Fe_4S_4(SR)_4]^{3-}$,[11-15] have demonstrated that these species are analogues of the 4-Fe clusters in Fd_{ox} and HP_{red}, and Fd_{red}, respectively. Recently, related selenium-containing clusters $[Fe_4X_4(YPh)_4]^{2-}$ (X, Y = S, Se), have been prepared in this[16] and another laboratory,[17] and their reduced forms generated in solution.[16] Among the characterized features of oxidized and reduced clusters are their structures and ^1H NMR spectral properties. The structures of $[Fe_4S_4(SPh)_4]^{2-}$,[7] $[Fe_4S_4(SPh)_4]^{3-}$,[13] $[Fe_4S_4(SCH_2Ph)_4]^{2-}$,[6] $[Fe_4S_4(SCH_2Ph)_4]^{3-}$,[15] and $[Fe_4Se_4(SPh)_4]^{2-}$ [16] are of particular pertinence to the present investigation and are summarized in Figure 1. In comprehensive studies of crystalline and solution-state properties of clusters, it has been demonstrated that the process

$$[Fe_4S_4(SR)_4]^{2-} \underset{-e^-}{\overset{+e^-}{\rightleftharpoons}} [Fe_4S_4(SR)_4]^{3-} \quad (2)$$

(I, compressed D_{2d}) (II, elongated D_{2d})

schematically depicted in Figure 1, represents the essential Fe_4S_4 core structural change accompanying electron transfer between oxidized and reduced clusters when extrinsic structural constraints are minimized.[13,14] The rather small structural differences between the two oxidation states suggest high electron self-exchange rates. In order to define exchange rates of clusters, measurements have been conducted for the pairs $[Fe_4S_4(S$-p-$C_6H_4Me)_4]^{2-,3-}$, $[Fe_4S_4(SCH_2Ph)_4]^{2-,3-}$, and $[Fe_4Se_4(S$-p-$C_6H_4Me)_4]^{2-,3-}$ in acetonitrile solution. Employment of NMR line shape analysis used for the kinetic measurements is facilitated by the large differences in ^1H chemical shifts, predominantly effected by isotropic contact interactions,[8-10,12] between the oxidized and reduced clusters. The results of this investigation, together with earlier measurements of comparative $Fd_{ox,red}/[Fe_4S_4(SR)_4]^{2-,3-}$ potentials[18] and the demonstration of process 2,[13,14] contribute to an emerging picture of the intrinsic operation of 4-Fe clusters in electron transfer, i.e., in the absence of modulating influences of protein structure.

0002-7863/80/1502-4350$01.00/0

Experimental Section

Preparation of Compounds. $(Et_4N)_2[Fe_4S_4(SCH_2Ph)_4]$,[6] $(Et_4N)_3[Fe_4S_4(SCH_2Ph)_4]$,[11] $(Me_4N)_2[Fe_4S_4(S\text{-}p\text{-}C_6H_4Me)_4]$,[8] and $(Me_4N)_3[Fe_4S_4(S\text{-}p\text{-}C_6H_4Me)_4]$[12] were prepared as previously described. Preparation and purification of new compounds were conducted under a pure dinitrogen atmosphere.

$(Me_4N)_2[Fe_4Se_4(S\text{-}p\text{-}C_6H_4Me)_4]$. This compound was obtained from the reaction of ferric chloride, sodium *p*-tolylthiolate, and selenium powder in methanol following the convenient procedure of Christou et al.[17] for the preparation of $[Fe_4Se_4(SPh)_4]^{2-}$. The crude product was purified by recrystallization from acetonitrile (λ_{max} 462 nm, ϵ_M 17 000 in acetonitrile). Anal. Calcd for $C_{36}H_{52}Fe_4N_2S_4Se_4$: C, 36.64; H, 4.44; Fe, 18.93; N, 2.37; S, 10.87; Se, 26.76. Found: C, 37.07; H, 4.43; Fe, 18.40; N, 2.31; S, 10.79; Se, 26.02.

$(Me_4N)_3[Fe_4Se_4(S\text{-}p\text{-}C_6H_4Me)_4]$. This compound was prepared by reduction of $(Me_4N)_2[Fe_4Se_4(S\text{-}p\text{-}C_6H_4Me)_4]$ with sodium acenaphthelenide in hexamethylphosphoramide using the procedure described elsewhere,[11,14] and purified by recrystallization from acetonitrile (λ_{max} 410 nm (ϵ_M 15 600), 268 (50 800)). Anal. Calcd for $C_{40}H_{64}Fe_4N_3S_4Se_4$: C, 38.30; H, 5.14; Fe, 17.81; N, 3.35; S, 10.22; Se, 25.18. Found: C, 38.36; H, 5.05; Fe, 17.69; N, 3.22; S, 10.13; Se, 25.09.

Preparation of Samples. Solutions of cluster salts for NMR investigation were prepared under an argon atmosphere in 99.0% acetonitrile-d_3 (Wilmad Glass Co.) containing 0.5 vol % Me_4Si, and sealed in NMR tubes under dynamic vacuum. Prior to use the solvent was dried over and distilled from calcium hydride, degassed under high vacuum, treated with excess $(Et_4N)_3[Fe_4S_4(SCH_2Ph)_4]$ (in order to remove oxidizing impurities), and vacuum distilled in a closed transfer tube. All solutions were used immediately after preparation.

^1H NMR Spectra. The 100-MHz spectra were recorded on instrumentation previously described.[12] Typical spectra were made by 1000–5000 acquisitions of 16 384 bits. Data were stored on a Diablo Model 31 magnetic disk system. The 360-MHz spectra were obtained on a Brüker HXS-360 spectrometer with an Oxford Instruments magnet and a Nicolet 1180 computer. Owing to the higher spectrometer sensitivity only 200 acquisitions were necessary per sample. Data were stored on a Diablo Model 44 magnetic disk system. For kinetic analyses the acquired data were digitized to 122.07 Hz/1024 bits for $[Fe_4X_4(S\text{-}p\text{-}C_6H_4Me)_4]^{2-,3-}$ (X = S, Se) at 100 MHz and 488.28 Hz/1024 bits for $[Fe_4S_4(S\text{-}p\text{-}C_6H_4Me)_4]^{2-,3-}$ and $[Fe_4S_4(SCH_2Ph)_4]^{2-,3-}$ at 360 and 100 MHz, respectively. Variable-temperature measurements were monitored by a Brüker temperature control unit.

NMR Data Processing. The rate analysis program DNMR used in this study was developed by D. Dalrymple of the Nicolet Technology Corp.[19] for use on the Nicolet 1180 computer. DNMR is a modified curve-fitting program that calculates a theoretical spectrum using a general line shape function for an AB system without spin coupling, derived from Bloch equations modified by Gutowsky and Holm,[20] but with the inclusion of transverse relaxation times:[21,22]

$$g(\omega) = \frac{\left\{P\left[1 + \tau\left(\frac{N_B}{T_{2A}} + \frac{N_A}{T_{2B}}\right)\right] + Q\left[R + \tau\left(\frac{1}{T_{2B}} - \frac{1}{T_{2A}}\right)\frac{\delta\omega}{2}\right]\right\}\omega_1 M_0}{P^2 + R^2 + \tau^2\left(\frac{1}{T_{2B}} - \frac{1}{T_{2A}}\right)^2\left(\frac{\delta\omega}{2}\right)^2 + 2R\tau\left(\frac{1}{T_{2B}} - \frac{1}{T_{2A}}\right)\frac{\delta\omega}{2}} \quad (3)$$

where

$$P = \tau\left[\frac{1}{T_{2A}T_{2B}} - (\Delta\omega)^2 + \left(\frac{\delta\omega}{2}\right)^2\right] + \frac{N_A}{T_{2A}} + \frac{N_B}{T_{2B}} \quad (4)$$

$$Q = \tau\left[\Delta\omega - \frac{\delta\omega}{2}(N_A - N_B)\right] \quad (5)$$

$$R = \Delta\omega\left[1 + \frac{\tau}{T_{2A}} + \frac{\tau}{T_{2B}}\right] + \frac{\delta\omega}{2}(N_A - N_B) \quad (6)$$

$$\tau = \frac{\tau_A\tau_B}{\tau_A + \tau_B} \quad (7)$$

and $g(\omega)$ = the transverse component of the resultant magnetic moment perpendicular to the rotating field H_1, which is proportional to the absorption intensity; $\delta\omega$ = difference of the intrinsic chemical shifts of sites A and B in the absence of exchange; $\Delta\omega$ = the frequency shift from the applied ω_1 of the two sites; N_A, N_B = mole fractions of sites A, B; T_{2A}, T_{2B} = transverse relaxation times of sites A, B in the absence of exchange; τ_A, τ_B = mean lifetime for sites A, B; ω_1 = applied rf field; M_0 = the equilibrium magnetization in the z direction.

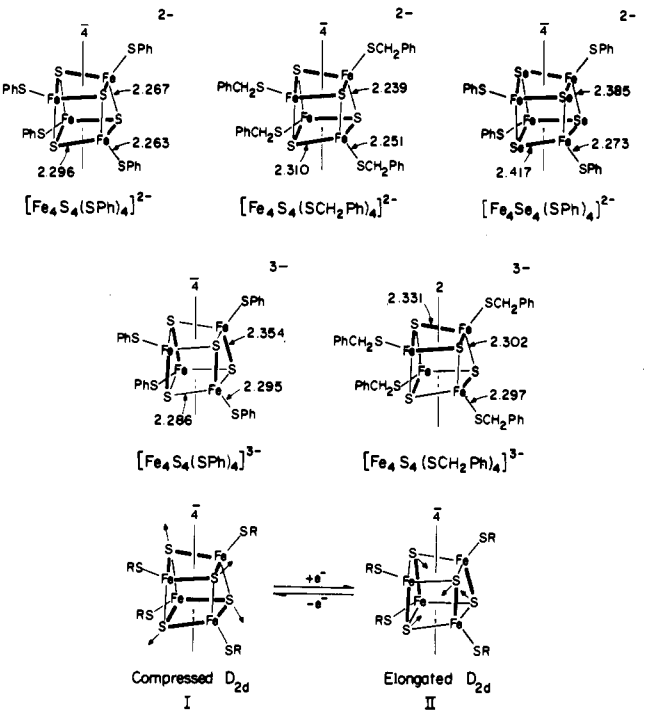

Figure 1. Structures of $[Fe_4S_4(SPh)_4]^{2-,3-}$, $[Fe_4S_4(SCH_2Ph)_4]^{2-,3-}$, and $[Fe_4Se_4(SPh)_4]^{2-}$ in the solid state, showing idealized core symmetry axes and mean values of Fe-SR and sets of longer (dark lines) and shorter Fe-S(Se) bond distances. Also shown is a simplified depiction of core structural changes accompanying electron transfer in solution.[13,14]

Solute mole fractions were evaluated from the equation

$$f_{av} = N_{2-}f_{2-} + N_{3-}f_{3-} \quad (8)$$

in which f_{av}, f_{2-}, and f_{3-} are the chemical shifts of the exchange-averaged resonance, pure $[Fe_4X_4(SR)_4]^{2-}$, and pure $[Fe_4X_4(SR)_4]^{3-}$ (X = S, Se), respectively. These results when checked were found to be within 1% of values calculated from solute weights. Transverse relaxation times ($T_2^{-1} = \pi\Delta\nu_{1/2}$) and the exact chemical-shift differences between sites A and B were evaluated from line widths ($\Delta\nu_{1/2}$) and chemical shifts of pure solutions of $[Fe_4X_4(SR)_4]^{2-,3-}$. The following resonances and data ($\Delta\nu_{1/2}$, Hz; δ, ppm from Me_4Si) were employed in the kinetic analyses (data refer to 100-MHz spectra unless otherwise noted): $[Fe_4S_4(S\text{-}p\text{-}C_6H_4Me)_4]^{2-}$, *m*-H, 7.21, 8.05 (10.9, 8.05 (at 360 MHz)); $[Fe_4S_4\text{-}(S\text{-}p\text{-}C_6H_4CH_3)_4]^{3-}$, *m*-H, 9.26, 10.40 (15.6, 10.40 (at 360 MHz)); $[Fe_4Se_4(S\text{-}p\text{-}C_6H_4Me)_4]^{2-}$, *m*-H, 6.65, 8.19; $[Fe_4Se_4(S\text{-}p\text{-}C_6H_4Me)_4]^{3-}$, *m*-H, 9.85, 11.62; $[Fe_4S_4(SCH_2Ph)_4]^{2-}$, CH_2, 47.9, 13.8; $[Fe_4S_4(SCH_2Ph)_4]^{3-}$, CH_2, 94.6, 35.5. Values of δ and $\Delta\nu_{1/2}$ were found to be independent of concentration except for apparent line widths of the extremely easily oxidized $[Fe_4S_4(SR)_4]^{3-}$ clusters, which were found to increase markedly at low concentrations. This behavior, which is illustrated in Figure 2 for one case, is likely due to oxidizing impurities in the solvent. Line-width variations with concentration could be reduced but not eliminated by solvent pretreatment with reduced cluster compounds. Consequently, exchange studies in each system were conducted in the fast exchange regime at $[Fe_4X_4(SR)_4]^{3-}$ concentrations (ca. 0.005–0.015 M) where the intrinsic line widths were essentially constant. These values were insignificantly different from those measured in saturated solutions of reduced clusters. Concentrations of $[Fe_4X_4(SR)_4]^{-2}$ were varied over a range up to ca. 20-fold larger or smaller than those of the reduced clusters. During data processing M_0 and τ were varied until the root mean square deviations between experimental exchange-broadened resonances and calculated line shapes were minimized. One result of the curve-fitting procedure is presented in Figure 3 as an example. As a check on the general line shape analysis procedure, exchange rates in one system were also evaluated using line-width determinations from a Lorentzian curve-

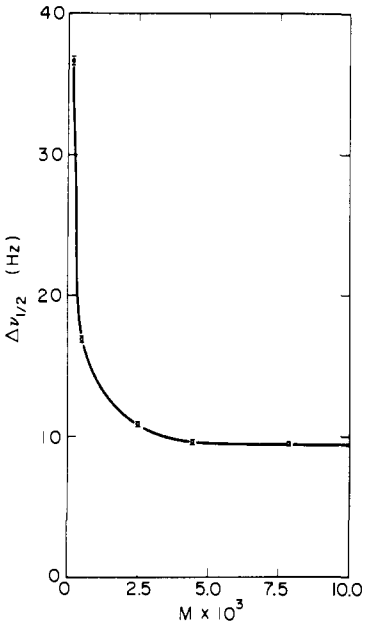

Figure 2. Dependence of *m*-H line widths of $[Fe_4S_4(S\text{-}p\text{-}C_6H_4Me)_4]^{3-}$ on concentration in CD_3CN solutions at 27 °C and 100 MHz. The solvent was pretreated with $(Et_4N)_3[Fe_4S_4(SCH_2Ph)_4]$ prior to use.

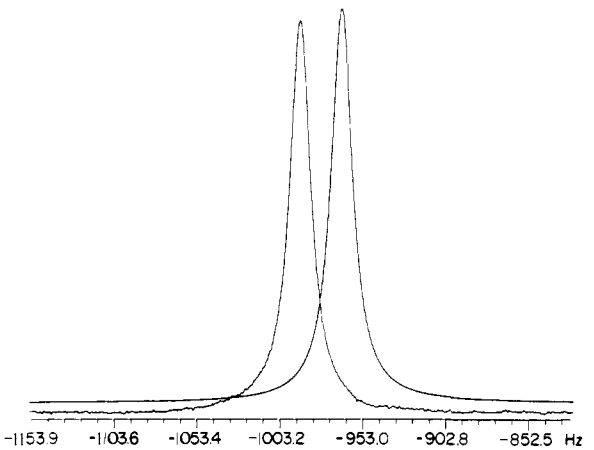

Figure 3. Comparison of experimental (left) and calculated (right) line shapes of the *m*-H resonance in the system $[Fe_4S_4(S\text{-}p\text{-}C_6H_4Me)_4]^{2-,3-}$ in acetonitrile solution at 300 K (N_{3-} = 0.804). The line-shape maxima are offset 20 Hz for display purposes.

fitting routine on the Nicolet 1180 computer. This method has been fully described elsewhere.[24]

Results and Discussion

Spectra of Oxidized and Reduced Clusters. Previous ^1H NMR studies of $[Fe_4S_4(SR)_4]^{2-}$ [8-10,12] and $[Fe_4S_4(SR)_4]^{3-}$ [12] complexes, in which oxidized and reduced clusters were examined separately, have shown that both species exhibit well-resolved spectra. These species are paramagnetic at ambient temperatures[25] and display resonances well shifted from those of diamagnetic RSH or RS^- references by isotropic magnetic interactions. Analysis of these spectra has demonstrated that the isotropic shifts, $(\Delta H/H_0)_{iso} = (\Delta H_0/H_0)_{obsd} - (\Delta H/H_0)_{dia}$, arise predominantly or exclusively from electron-nuclear hyperfine contact interactions.[8,12] The spectra of $[Fe_4Se_4(S\text{-}p\text{-}C_6H_4Me)_4]^{2-,3-}$, set out in Figure 4, together with the tabulated isotropic shifts of $[Fe_4Se_4(SPh)_4]^{2-}$,[17] are consistent with dominant contact shifts resulting from RS → Fe_4Se_4 core antiparallel spin transfer. Shifts of *o*-H and *p*-H are upfield (positive), the *m*-H shifts are downfield (negative), and the sign of the shifts reverses upon *p*-H/*p*-Me substitution. The same behavior has been observed for the analogous $[Fe_4S_4(SR)_4]^{2-,3-}$ clusters; isotropic shifts of $[Fe_4X_4(SR)_4]^{2-,3-}$ species are compared in Table I. The larger shifts of $[Fe_4Se_4(SR)_4]^{2-}$ vs. $[Fe_4S_4(SR)_4]^{2-}$ are consistent with the larger magnetic moment of the former[25] (μ_t = 2.47 μ_B, R = Ph, 299 K[16]), a property that presumably applies to the corresponding reduced clusters as well. A notable feature of the spectrum of $[Fe_4Se_4(S\text{-}p\text{-}C_6H_4Me)_4]^{3-}$ when examined at 360 MHz is observation of the broad *o*-H signal at +0.18 ppm. This signal was not resolved in the spectrum of the corresponding Fe_4S_4 complex at 100 MHz.[12] Remeasurement of the latter at 360 MHz located the *o*-H resonance at −2.35 ppm, resulting in a correction (Table I) of the previously estimated[12] isotropic shift.

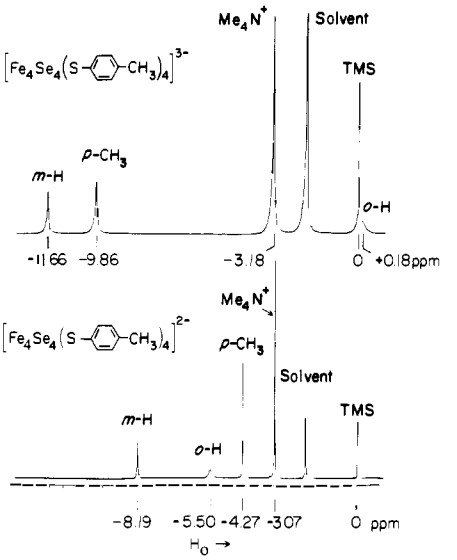

Figure 4. ^1H FT NMR spectra (360 MHz) of Me_4N^+ salts of $[Fe_4Se_4(S\text{-}p\text{-}C_6H_4Me)_4]^{2-}$ (lower) and $[Fe_4Se_4(S\text{-}p\text{-}C_6H_4Me)_4]^{3-}$ (upper) in CD_3CN solutions at ~23 °C. Signal assignments are indicated.

Table I. Isotropic Shifts of Oxidized and Reduced Clusters in CD_3CN Solution

cluster	position	$(\Delta H/H_0)_{iso}$,[a] ppm	ref
$[Fe_4S_4(S\text{-}p\text{-}C_6H_4Me)_4]^{2-}$	*o*-H	+1.28	8, 12
	m-H	−0.91	
	p-Me	−1.63	
$[Fe_4Se_4(S\text{-}p\text{-}C_6H_4Me)_4]^{2-}$ [c]	*o*-H	+1.60	this work
	m-H	−1.09	
	p-Me	−1.99	
$[Fe_4S_4(S\text{-}p\text{-}C_6H_4Me)_4]^{3-}$	*o*-H	+4.75	12
	m-H	−3.25	
	p-Me	−5.20	
$[Fe_4Se_4(S\text{-}p\text{-}C_6H_4Me)_4]^{3-}$	*o*-H	+7.38	this work
	m-H	−4.56	
	p-Me	−7.58	
$[Fe_4S_4(SCH_2Ph)_4]^{2-}$	CH_2	−10.2[b]	8, 12
$[Fe_4S_4(SCH_2Ph)_4]^{3-}$	CH_2	−30.8	12

[a] Values at 299-300 K unless otherwise noted; $(\Delta H/H_0)_{iso} = (\Delta H/H_0)_{obsd} - (\Delta H/H_0)_{dia}$ (see ref 8 and 12). [b] 295 K. [c] Shifts of $[Fe_4Se_4(SPh)_4]^{2-}$ in $Me_2SO\text{-}d_6$:[17] *o*-H, +1.98; *m*-H, −1.15; *p*-H, +2.49 ppm (30 °C).

Electron Exchange Kinetics. The rates of the electron self-exchange reaction

$$*[Fe_4X_4(SR)_4]^{2-} + [Fe_4X_4(SR)_4]^{3-} \rightleftharpoons *[Fe_4X_4(SR)_4]^{3-} + [Fe_4X_4(SR)_4]^{2-} \quad (9)$$

were determined for three pairs of oxidized and reduced clusters, $[Fe_4S_4(S\text{-}p\text{-}C_6H_4Me)_4]^{2-,3-}$, $[Fe_4S_4(SCH_2-$

Table II. Electron Self-Exchange Kinetic Data for $[Fe_4X_4(SR)_4]^{2-,3-}$ and Fe-S Proteins

species	T, K	k, M^{-1} s^{-1}	ref
$[Fe_4S_4(SCH_2Ph)_4]^{2-,3-}$	300	$2.4 \pm 0.2 \times 10^6$ [b,d]	*a*
$[Fe_4S_4(S\text{-}p\text{-}C_6H_4Me)_4]^{2-,3-}$	301	$2.8 \times 0.3 \times 10^6$ [c,d] $\Delta G^{\ddagger}_{298K} = 8.7$ kcal/mol $\Delta H = 3.6$ kcal/mol $\Delta S = -17$ eu	*a*
	300	$5.8 \pm 0.6 \times 10^6$ [b,d]	*a*
$[Fe_4Se_4(S\text{-}p\text{-}C_6H_4Me)_4]^{2-,3-}$	304	$9.7 \times 0.9 \times 10^6$ [b,d]	*a*
C. pasteurianum $Rd_{ox,red}$	298	10^8-10^9 [e,f]	41
spinach $Fd_{ox,red}$	298	1.7×10^{-3} [e,g]	42
Chromatium $HP_{ox,red}$	298	1.3×10^{-2} [e,g]	43

[a] This work. [b,c] Determined at [b]100 MHz, [c]360 MHz. [d] Acetonitrile solution. [e] Aqueous buffer. [f] Uncorrected for reagent electrostatic effects. Estimated activation parameters: $\Delta H^{\ddagger} \sim 0$ kcal/mol, $\Delta S^{\ddagger} \sim -18$ eu. [g] Electrostatics-corrected value for reaction with Fe(EDTA) reagent.

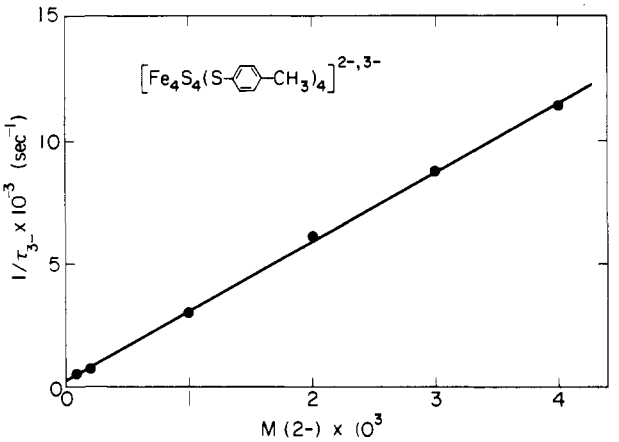

Figure 5. Plot of $1/\tau_{3-}$ vs. the concentration of the oxidized cluster for the system $[Fe_4S_4(S\text{-}p\text{-}C_6H_4Me)_4]^{2-,3-}$ in acetonitrile solution at 28 °C. The concentration of the reduced cluster is 5.91 mM. Line shapes measured at 360 MHz were used.

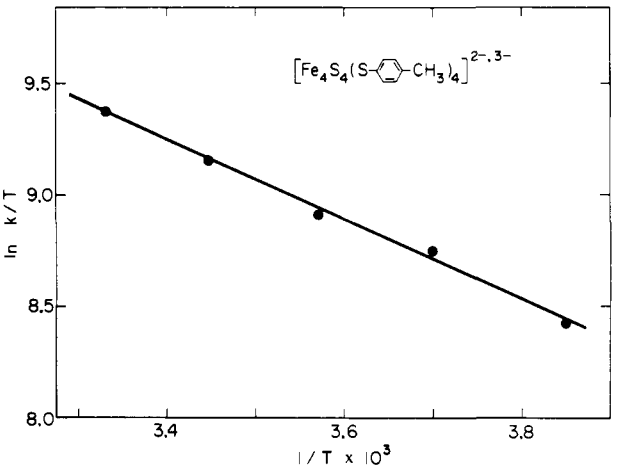

Figure 6. Temperature dependence of the electron exchange rate constants of the system $[Fe_4S_4(S\text{-}p\text{-}C_6H_4Me)_4]^{2-,3-}$ in acetonitrile solution over the interval 260-300 K.

Ph)$_4]^{2-,3-}$, and $[Fe_4Se_4(S\text{-}p\text{-}C_6H_4Me)_4]^{2-,3-}$, in acetonitrile solution by use of the general line shape analysis procedure. At the concentrations employed all systems exhibited exchange-broadened resonances (e.g., Figure 3) whose chemical shifts followed eq 8. Variation of the concentrations of reduced cluster, [3−], and oxidized cluster, [2−], indicated that all systems obeyed the second-order kinetics

$$-\mathrm{d}[3-]/\mathrm{d}t = k[3-][2-] \qquad (10)$$

Here $1/\tau_{3-} = k[2-]$ and $1/\tau_{2-} = k[3-]$. A plot of $1/\tau_{3-}$ vs. [2−] illustrating second-order behavior is shown in Figure 5. In such plots the data points were analyzed by eq 3 and fit using a linear least-squares analysis; rate constants, summarized in Table II, were evaluated from slopes. For the system $[Fe_4S_4(SCH_2Ph)_4]^{2-,3-}$ the rate constant was also evaluated by a Lorentzian curve-fitting procedure. The result, $k = 2.1 \times 10^6$ M^{-1} s^{-1}, is in good agreement with that ($k = 2.4 \times 10^6$ M^{-1} s^{-1}) obtained from the general line shape method.

Activation parameters were determined for one system, $[Fe_4S_4(S\text{-}p\text{-}C_6H_4Me)_4]^{2-,3-}$, whose rate constant was evaluated from spectra determined at 360 MHz. Parameters were evaluated from eq 11, a plot of which is shown in Figure 6, and are collected in Table II. These values give a calculated rate constant of 2.9×10^6 M^{-1} s^{-1} at 301 K.

$$k = \frac{k_B T}{h} \exp\left[\frac{\Delta S^{\ddagger}}{R} - \frac{\Delta H^{\ddagger}}{RT}\right] \qquad (11)$$

A. Rate Constants. Values of the second-order rate constants for the three reactions (9) occur in the interval 10^6–10^7 M^{-1} s^{-1} at 300—304 K, marking them to be among the faster inorganic electron self-exchange systems currently characterized. Systems with $k \gtrsim 10^6$ M^{-1} s^{-1} are uncommon; examples include $[Fe(phen)_3]^{2+,3+}$,[26] $[M(bpy)_3]^{2+,3+}$ (M = Fe, Ru),[26,27] Cu(II,III)-peptide complexes,[28] and $[Fe(S_2CNMe_2)_3]^{0,+}$.[29] A tabulation of self-exchange rate constants of a number of other inorganic complexes is available elsewhere.[30]

The rate constants in Table II for the reactions (9) vary at the extremes by a factor of only 4, suggesting that these reactions take place by essentially the same mechanism. Inasmuch as separate experiments have shown that RS/R′S and S/Se exchange between clusters is slower than electron transfer, the reactions proceed by an outer-sphere pathway. Variation of cluster atom X = S, Se in $[Fe_4X_4(S\text{-}p\text{-}C_6H_4Me)_4]^{2-,3-}$ gave rate constants which differ by a factor of 1.7, showing little if any effect of the larger radial extension of Se orbitals in the electron-exchange process. Similarly, limited variation of substituent R = Ph, CH_2Ph with X = S afforded rate constants measured under the same conditions which differ by a factor of only 2.4. Such differences are too small for meaningful interpretation

B. Activation Parameters. The values of $\Delta G^{\ddagger}$, $\Delta H^{\ddagger}$, and $\Delta S^{\ddagger}$ in Table II for the system $[Fe_4S_4(S\text{-}p\text{-}C_6H_4Me)_4]^{2-,3-}$ are quite similar to those for $[Fe(phen)_3]^{2+,3+}$ and $[M(bpy)_3]^{2+,3+}$ (M = Fe, Ru) determined in acetonitrile solution.[26] In particular, $\Delta S^{\ddagger}$ values (−15 to −22 eu) for the latter three systems, whose fast electron exchange reactions ($k \sim 10^6$–10^7 M^{-1} s^{-1}) unquestionably involve a bimolecular outer-sphere mechanism, are closely comparable to $\Delta S^{\ddagger} = -17$ eu found for cluster electron exchange.

Factors affecting electron-exchange rates of inorganic systems have been delineated.[31,32] Among these, small values of the "inner shell" reorganization energy $\Delta G^{\ddagger}_{reorg} \simeq \Delta E^{\ddagger}_{reorg}$ appear to be consistently associated with relatively fast self-exchange rates ($k \gtrsim 10^2$ M^{-1} s^{-1}).[33] This energy,

which is that required to adjust reactants to identical nuclear configurations upon the event of electron transfer, can be estimated for reaction 9. From the results summarized in Figure 1 the *principal* structural change as a consequence of electron transfer, process 2, is elongation and compression of the Fe_4S_4 core along the $\bar{4}$ axis. This process has been shown to apply in solution even if the core structure of a reduced cluster is not tetragonal in the solid state;[13,14] cores of all oxidized clusters exhibit a nearly uniform compressed tetragonal structure. For $[Fe_4S_4(SPh)_4]^{2-,3-}$ the mean Fe-S bond distances approximately parallel to the $\bar{4}$ axis are altered by 0.087 Å, whereas those roughly perpendicular to this axis change by only 0.010 Å. The free energy of core reorganization is approximated by

$$\Delta G^{\ddagger}_{reorg} = 2k_{2-}(r_{2-} - r_{\pm})^2 + 2k_{3-}(r_{3-} - r_{\pm})^2 \quad (12)$$

in which the k and r values are Fe-S stretching force constants and mean bond distances of the four bonds approximately parallel to the $\bar{4}$ axis, respectively, and $r_{\pm}$ is the corresponding bond distance in the transition state. From $(\partial \Delta G^{\ddagger}_{reorg}/\partial r_{\pm}) = 0$, $r_{\pm} = (k_{2-}r_{2-} + k_{3-}r_{3-})/(k_{2-} + k_{3-})$. Using $\nu_{FeS} = 343$ and 341 cm^{-1} for $[Fe_4S_4(SPh)_4]^{2-}$ and $[Fe_4S_4(SPh)_4]^{3-}$,[34] respectively, and the bond distances for these clusters in Figure 1, $r_{\pm} = 2.31$ Å and $\Delta G^{\ddagger}_{reorg} = 1.5$ kcal/mol. While this calculation is obviously crude,[35] the results imply only a small contribution to the total free energy of activation from core structural rearrangement[36] in attaining the transition state, which has been proposed to involve clusters with essentially cubic (T_d) core geometry.[13]

Ferredoxin Electron Self-Exchange. A. Intrinsic Rates. As discussed elsewhere,[4,5] a significant advantage of properly constructed analogues of protein sites is that their properties are those intrinsic to the site; i.e., they are unmodified by extrinsic influences of protein structure and environment. With the analogues $[Fe_4S_4(SR)_4]^{2-,3-}$, ideally R = *n*-alkyl in order to simulate closely cysteinate binding in $[Fe_4S_4(S\text{-}Cys)_4]$ protein sites. Some properties, e.g., structures of oxidized clusters[6,7,37] (Figure 1), are rather insensitive to the nature of R, whereas others such as redox potentials[9,38] are not. Unfortunately, the extreme oxidative instability of reduced clusters with R = *n*-alkyl ($E_{1/2} < -1.3$ V vs. SCE in DMF[38]) has thus far prevented their isolation in analytical purity.[14] For this reason the present kinetic studies have been performed with certain of those clusters (R = CH_2Ph, *p*-C_6H_4Me) isolable in pure form in both oxidized and reduced states. Accurate models constructed from crystallographic coordinates[6,7] reveal that with R = CH_2Ph the phenyl ring may closely approach the Fe_4S_4 core in conformations edgewise or nearly parallel (separation ~2.5 Å) to a Fe_2S_2 face. No such close approaches are possible with R = Ph, which, however, lacks a potentially insulating methylene group. These factors, together with the demonstration of unpaired spin delocalization over phenyl rings in $[Fe_4S_4(SR)_4]^{2-,3-}$ (R = CH_2Ph, Ph, C_6H_4Me),[8,12] may act to accelerate electron transfer relative to the R = *n*-alkyl case.[39] Hence, the rate constants in Table II may not be the actual intrinsic values of protein sites. These are, however, the best available estimates of these values and are treated as such in the following discussion.

B. Protein Rates. No electron self-exchange rates of Fe-S proteins have been directly measured. The estimates in Table II are based on experimental cross reaction rates and application of relative Marcus theory,[30,41-43] and must be cautiously interpreted owing to their dependence on the inorganic redox partner in the cross reactions. They do suggest the redox site kinetic accessibility order rubredoxin (Rd) > spinach Fd ~ HP, consistent with the positions of the 1-Fe Rd site near the protein surface[44a] and the 4-Fe site of HP buried in the protein interior.[44b] Reorganization energies of the $[Fe(S\text{-}Cys)_4]^{1-,2-}$ site in Rd may now be estimated from protein EXAFS[45a] and analogue structural results[45b] and the resonance Raman spectrum of Rd_{ox}.[45c] From eq 12 $\Delta G^{\ddagger}_{reorg} \lesssim 1.3$ kcal/mol if $k_{1-} \simeq k_{2-}$.

None of the rate-constant estimates in Table II involves the Fd_{ox}/Fd_{red} couple (1). This is the operative couple in *Bacillus polymyxa* Fd 1 (mol wt ~9000), half-reduced solutions of which are reported to exhibit NMR spectra that are superpositions of those of the oxidized and reduced proteins.[46] In contrast, partially reduced clostridial-type ferredoxins, which contain two 4-Fe sites separated by ~12 Å[3a] in monomeric proteins of molecular weights ~6200 and utilize couple (1), give exchange-averaged ^1H[47] and ^{13}C[48] NMR spectra. For *B. polymyxa* Fd 1 slow exchange system we very crudely estimate $k \lesssim 10^3$ M^{-1} s^{-1} as an upper limit. Based on the analogue rate constants of 10^6–10^7 M^{-1} s^{-1} it is highly unlikely that decreased rate of protein self-exchange arises from intrinsically slow reactions of the sites themselves. The rate decrease of $\gtrsim 10^3$ M^{-1} s^{-1} compared to the analogues is more reasonably interpreted as a rough measure of kinetically retarding steric influences of protein structure in the transition state and whatever effects this structure may have on the mechanism of electron transfer.[49] As suggested earlier,[46,47b] the slow-exchange spectrum of *B. polymyxa* Fd I and the exchange-averaged spectra of clostridial-type Fd's may indicate a component of intramolecular electron exchange in the latter proteins. If anything, the very fast exchange rates determined in this work enhance the possibility of intramolecular exchange,[50] particularly upon noting that certain cysteinate sulfur atoms of different sites in *P. aerogenes* Fd_{ox} can approach each other more closely than 12 Å.[3a] However, the position of the 4-Fe site in *B. polymyxa* Fd 1 is unknown, the two sites in *P. aerogenes* Fd_{ox} are not deeply buried within the protein structure,[3a] and the necessary measurements of concentration dependence of NMR spectra required to sort out inter- vs. intramolecular exchange effects on line shapes have not been reported.

Acknowledgment. This research was supported by NIH Grant GM 22352. C.L.C. acknowledges an award from Sigma Xi. Facilities at the Stanford Magnetic Resonance Laboratory are supported by NIH Grant RR-00711 and NSF Grant GR-23633.

References and Notes

(1) Postdoctoral Fellow, American Cancer Society, 1977–1979.
(2) (a) G. Palmer in "The Enzymes", Vol. XII, Part B, 3rd ed., P. D. Boyer, Ed., Academic Press, New York, 1975, pp 1–56; (b) D. O. Hall, R. Cammack, and K. K. Rao, in "Iron in Biochemistry and Medicine", A. Jacobs and M. Worwood, Ed., Academic Press, New York, 1974, Chapter 8.
(3) (a) E. T. Adman, L. C. Sieker, and L. H. Jensen, *J. Biol. Chem.*, **248**, 3987 (1973); **251**, 3801 (1976); (b) C. W. Carter, Jr., in "Iron-Sulfur Proteins", Vol. 3, W. Lovenberg, Ed., Academic Press, New York, 1977, Chapter 6; (c) C. W. Carter, Jr., *J. Biol. Chem.*, **252**, 7802 (1977).
(4) R. H. Holm and J. A. Ibers in ref 3b, Chapter 7.
(5) R. H. Holm, *Acc. Chem. Res.*, **10**, 427 (1977).
(6) B. A. Averill, T. Herskovitz, R. H. Holm, and J. A. Ibers, *J. Am. Chem. Soc.*, **95**, 3523 (1973).
(7) L. Que, Jr., M. A. Bobrik, J. A. Ibers, and R. H. Holm, *J. Am. Chem. Soc.*, **96**, 4168 (1974).
(8) R. H. Holm, W. D. Phillips, B. A. Averill, J. J. Mayerle, and T. Herskovitz, *J. Am. Chem. Soc.*, **96**, 2109 (1974).
(9) L. Que, Jr., J. R. Anglin, M. A. Bobrik, A. Davison, and R. H. Holm, *J. Am. Chem. Soc.*, **96**, 6042 (1974).
(10) G. B. Wong, D. M. Kurtz, Jr., R. H. Holm, L. E. Mortenson, and R. G. Upchurch, *J. Am. Chem. Soc.*, **101**, 3078 (1979).
(11) J. Cambray, R. W. Lane, A. G. Wedd, R. W. Johnson, and R. H. Holm, *Inorg. Chem.*, **16**, 2565 (1977).
(12) J. G. Reynolds, E. J. Laskowski, and R. H. Holm, *J. Am. Chem. Soc.*, **100**, 5315 (1978).
(13) E. J. Laskowski, R. B. Frankel, W. O. Gillum, G. C. Papaefthymiou, J. Renaud, J. A. Ibers, and R. H. Holm, *J. Am. Chem. Soc.*, **100**, 5322 (1978).
(14) E. J. Laskowski, J. G. Reynolds, R. B. Frankel, S. Foner, G. C. Papaefthymiou, and R. H. Holm, *J. Am. Chem. Soc.*, **101**, 6562 (1979).
(15) J. M. Berg, K. O. Hodgson, and R. H. Holm, *J. Am. Chem. Soc.*, **101**, 4586 (1979).
(16) M. A. Bobrik, E. J. Laskowski, R. W. Johnson, W. O. Gillum, J. M. Berg, K. O. Hodgson, and R. H. Holm, *Inorg. Chem.*, **17**, 1402 (1978).
(17) G. Christou, B. Ridge, and H. N. Rydon, *J. Chem. Soc., Dalton Trans.*, 1423 (1978).

(18) C. L. Hill, J. Renaud, R. H. Holm, and L. E. Mortenson, *J. Am. Chem. Soc.*, **99**, 2549 (1977).
(19) Nicolet Technology Corp., Mountain View, Calif. 94041.
(20) H. S. Gutowsky and C. H. Holm, *J. Chem. Phys.*, **25**, 1228 (1956).
(21) Cf., e.g., K. C. Williams and T. L. Brown, *J. Am. Chem. Soc.*, **88**, 4134 (1966).
(22) It is noted that the line shape eq 3 exhibits limitations when the two site populations become very unequal ($\gtrsim 10/1$),[23] a situation which was avoided in the large majority of measurements used to determine rate data.
(23) F. A. L. Anet and V. J. Basus, *J. Magn. Reson.*, **32**, 339 (1978).
(24) A. Allerhand, H. S. Gutowsky, J. Jones, and R. A. Meinzer, *J. Am. Chem. Soc.*, **88**, 3185 (1966); L. H. Piette and W. A. Anderson, *J. Chem. Phys.*, **30**, 899 (1959).
(25) Typical magnetic moments per tetranuclear (4-Fe) unit at ~300 K are μ_t = 2.0–2.2 μ_B for $[Fe_4S_4(SR)_4]^{2-}$ in the solution and solid state[8,13] and μ_t = 3.6–3.8 μ_B for $[Fe_4S_4(SR)_4]^{3-}$ in solution.[12]
(26) M-S. Chan and A. C. Wahl, *J. Phys. Chem.*, **82**, 2542 (1978).
(27) G. M. Brown and N. Sutin, *J. Am. Chem. Soc.*, **101**, 883 (1979).
(28) G. D. Owens, K. L. Chellappa, and D. W. Margerum, *Inorg. Chem.*, **18**, 960 (1979).
(29) M. C. Palazzotto and L. H. Pignolet, *Inorg. Chem.*, **13**, 1781 (1974).
(30) S. Wherland and H. B. Gray in "Biological Aspects of Inorganic Chemistry", A. W. Addison, W. R. Cullen, D. Dolphin, and B. R. James, Ed., Wiley, New York, 1977, pp 289–368.
(31) W. L. Reynolds and R. W. Lumry, "Mechanisms of Electron Transfer", Ronald Press, New York, 1966.
(32) N. Sutin in "Inorganic Biochemistry", Vol. 2, G. L. Eichhorn, Ed., Elsevier, Amsterdam, 1973, Chapter 19.
(33) For consideration of several such cases, cf., e.g., H. C. Stynes and J. A. Ibers, *Inorg. Chem.*, **10**, 2304 (1971).
(34) T. G. Spiro, private communication.
(35) Other than the obviously simplifying assumption of Fe–S bonds as harmonic oscillators, the calculation is rendered approximate by the fact that the ~340-cm^{-1} bands do not arise from pure Fe–S stretching mode(s). Better estimates of stretching force constants may become available from a vibrational analysis of the clusters.[34]
(36) If the difference in terminal Fe–S distances in $[Fe_4S_4(SPh)_4]^{2-,3-}$ (0.032 Å, Figure 1) is taken into account and $\nu_{FeS} \simeq 430$ cm^{-1} for both oxidized and reduced clusters,[34] the contribution to $\Delta G^{\ddagger}_{reorg}$ from rearrangement of these distances is $\lesssim 0.4$ kcal/mol.
(37) H. L. Carrell, J. P. Glusker, R. Job, and T. C. Bruice, *J. Am. Chem. Soc.*, **99**, 3683 (1977).
(38) B. V. DePamphilis, B. A. Averill, T. Herskovitz, L. Que, Jr., and R. H. Holm, *J. Am. Chem. Soc.*, **96**, 4159 (1974).
(39) Rate enhancements in inorganic complexes upon replacing saturated with conjugated ligands are well recognized. Rate-constant ratios for the following pairs are examples: $[Ru(bpy)_3]^{2+,3+}/[Ru(NH_3)_6]^{2+,3+}$, ~$10^5$;[27] $[Co(phen)_3]^{2+,3+}/[Co(NH_3)_{6-n}(H_2O)_n]^{2+,3+}$ $\lesssim 10^{12}$ [30] (D. R. Stranks, *Discuss. Faraday Soc.*, **29**, 116 (1960)). However, as opposed to the $[Fe_4X_4(SR)_4]^{2-,3-}$ cases, the conjugated ligands are directly bonded to the metal. Note also that early suggestions of an electron-transfer function of aromatic residues positioned near to 4-Fe redox sites of clostridial-type ferredoxins have been voided. Such residues have little effect on rates of reduction in biological assays or on redox potentials.[40] These residues less closely approach the protein site cores (3.5–4 Å[3a]) than is possible in certain conformations of $[Fe_4S_4(SCH_2Ph)_4]^{2-,3-}$.
(40) E. T. Lode, C. L. Murray, W. V. Sweeney, and J. C. Rabinowitz, *Proc. Natl. Acad. Sci. U.S.A.*, **71**, 1361 (1974); E. T. Lode, C. L. Murray, and J. C. Rabinowitz, *Biochem. Biophys. Res. Commun.*, **61**, 163 (1974); *J. Biol. Chem.*, **251**, 1683 (1976).
(41) C. A. Jacks, L. E. Bennett, W. N. Raymond, and W. Lovenberg, *Proc. Natl. Acad. Sci. U.S.A.*, **71**, 118 (1974).
(42) J. Rawlings, S. Wherland, and H. B. Gray, *J. Am. Chem. Soc.*, **99**, 1968 (1977).
(43) D. Cummins and H. B. Gray, *J. Am. Chem. Soc.*, **99**, 5158 (1977).
(44) (a) L. H. Jensen in ref 3b, Vol. II, 1973, Chapter 4; E. T. Adman, L. C. Sieker, L. H. Jensen, M. Bruschi, and J. LeGall, *J. Mol. Biol.*, **112**, 113 (1977); (b) C. W. Carter, Jr., J. Kraut, S. T. Freer, N. Xuong, R. A. Alden, and R. G. Bartsch, *J. Biol. Chem.*, **249**, 4212 (1974).
(45) (a) R. G. Shulman, P. Eisenberger, B. K. Teo, B. M. Kincaid, and G. S. Brown, *J. Mol. Biol.*, **124**, 305 (1978); (b) R. W. Lane, J. A. Ibers, R. B. Frankel, G. C. Papaefthymiou, and R. H. Holm, *J. Am. Chem. Soc.*, **99**, 84 (1977); (c) T. V. Long, II, T. M. Loehr, J. R. Allkins, and W. Lovenberg, *ibid.*, **93**, 1809 (1971).
(46) W. D. Phillips, C. C. McDonald, N. A. Stombaugh, and W. H. Orme-Johnson, *Proc. Natl. Acad. Sci. U.S.A.*, **71**, 140 (1974).
(47) (a) M. Poe, W. D. Phillips, C. C. McDonald, and W. Lovenberg, *Proc. Natl. Acad. Sci. U.S.A.*, **65**, 797 (1970); (b) M. Poe, W. D. Phillips, C. C. McDonald. and W. H. Orme-Johnson, *Biochem. Biophys. Res. Commun.*, **42**, 705 (1971); (c) E. L. Packer, W. V. Sweeney, J. C. Rabinowitz, H. Sternlicht, and E. N. Shaw, *J. Biol. Chem.*, **252**, 2245 (1977).
(48) E. L. Packer, H. Sternlicht, E. T. Lode, and J. C. Rabinowitz, *J. Biol. Chem.*, **250**, 2062 (1975).
(49) Slow exchange on the ^1H NMR time scale has also been reported between HP_{ox} and HP_{red} from *Chromatium*.[46] Because the redox site is ~4 Å from the protein surface, the "slow" rate would appear to be a consequence of protein structure provided that the intrinsic $[Fe_4S_4(S\text{-}Cys)_4]^{1-,2-}$ self-exchange rate is comparable to those for the analogue 2−/3− systems in Table II.
(50) Recent pulse radiolysis experiments have detected a two-stage reduction of *Clostridium pasteurianum* 8-Fe Fd_{ox} by solvated electrons.[51] The very fast initial reduction ($k_1 = 3.4 \times 10^{10}$ M^{-1} s^{-1}) is followed by a slower, apparently intramolecular process ($k_2 = 1.1 \times 10^3$ s^{-1}). It is not clear whether the latter corresponds to electron transfer from one 4-Fe site to the other or from a reduced phenyl ring of a Phe or Tyr residue to a 4-Fe site.[51]
(51) J. Butler, R. A. Henderson, F. A. Armstrong, and A. G. Sykes, *Biochem. J.*, **183**, 471 (1979).

Hydroboration Reactions with 6-Thia-*nido*-decaborane(11)

B. J. Meneghelli, M. Bower, N. Canter, and R. W. Rudolph*

Contribution from the Department of Chemistry, The University of Michigan, Ann Arbor, Michigan 48109. *Received November 7, 1979*

Abstract: Alkenes and alkynes undergo a facile hydroboration reaction with 6-SB_9H_{11}. Alkenes give 9-R-6-SB_9H_{10} products where R = alkyl. Those alkenes investigated were ethylene, 1-octene, cyclohexene, cyclopentadiene, styrene, and 1-methyl-1-cyclohexene. Alkynes give 9-R′-6-SB_9H_{10} products where R′ = alkenyl. In the case of acetylene a double hydroboration occurs to give 9,9′-CH_3CH-(6-SB_9H_{10})$_2$. Those alkynes investigated were acetylene, diphenylacetylene, phenylacetylene, and 3-hexyne. Attachment of the organic moiety to the 9 position of the 6-SB_9H_{10} cage was established by ^{11}B NMR. The ^{13}C and ^1H NMR spectra and mass spectra were also consistent with hydroboration. Oxidation of the organothiaboranes by alkaline peroxide gave the expected ketone or alcohol for most cases. The observation of *trans*-2-methylcyclohexanol after oxidation of the 1-methyl-1-cyclohexene hydroboration product indicates that the hydroboration is a regiospecific anti-Markownikoff syn addition. A possible mechanism is discussed. Pyrolysis (400–450 °C) of the nido 9-R-6-SB_9H_{10} molecules gives the corresponding closo derivative as a mixture of 2-, 6-, and 10-R-1-SB_9H_8 isomers. The interaction of aldehydes and ketones with 6-SB_9H_{11} is more complex and involves degradative hydroboration.

Introduction

A facile and clean hydroboration reaction for a nonpyrophoric, polyhedral borane was not demonstrated until our recent report concerning the reactions of 6-SB_9H_{11}.[1] For instance, it is necessary to subject a mixture of the pyrophoric pentaborane(9) and an olefin to 150 °C in order to form 2-alkyl-B_5H_8 species (alkyl = *n*-Bu, *sec*-Bu, *i*-Bu, Et).[2] Pentaborane(11) hydroborates ethylene,[3] but the reaction is not clean and B_5H_{11} is even more difficult to prepare and handle than B_4H_{10} or B_5H_9. The reactions of B_5H_{11} and B_4H_{10} with acetylenes lead to complex product mixes which include carbaboranes[4] (i.e., some carbon is incorporated into the cage). In contrast, the hydroboration described here involves the easily handled and readily prepared 6-thia-*nido*-decaborane(11).

0002-7863/80/1502-4355$01.00/0